model of the head," *Med. Biol. Eng. Comp.*, vol. 23, pp. 36–37, 1985.
[9] M. S. Hämäläinen and J. Sarvas, "Realistic conductivity geometry model of the human head for interpretation of neuromagnetic data," *IEEE Trans. Biomed. Eng.*, vol. 36, pp. 165–171, Feb. 1989.
[10] A. van Oosterom and J. Strackee, "The solid angle of a plane triangle," *IEEE Trans. Biomed. Eng.*, vol. BME-30, pp. 125–126, 1983.
[11] M. S. Lynn and W. P. Timlake, "The use of multiple deflations in the numerical solution of singular systems of equations with applications to potential theory," *SIAM. J. Numer. Anal.*, vol. 5, pp. 303–322, 1968.
[12] T. Kuwahara and T. Takeda, "An effective analysis for three dimensional boundary element method using analytically integrated higher order elements," *Trans. IEE Japan*, vol. 107A, pp. 275–281, 1987, (In Japanese).
[13] ——, "A formula of boundary integral for potential problem and its consideration," in *Proc. First. Japan-China Symp. Boundary Element Methods Theory Appl.*, M. Tanaka and Q. H. Du, Eds. New York: Pergamon, 1987, pp. 47–55.
[14] H. L. G. Pina, J. L. M. Fernandes, and C. A. Brebbia, "Some numerical integration formulae over triangles and squares with a $1/R$ singularity," *Appl. Math. Modelling*, vol. 5, pp. 209–211, 1981.
[15] M. W. Yao, "Improved Gaussian quadratures for bounary element integrals," *Eng. Anal. Bound. Elem.*, vol. 6, no. 2, pp. 108–113, 1989.
[16] M. H. Alliabadi and W. S. Hall, "The regularisation transformation integration method for boundary element kernels. Comparison with series expansion and weighed Gaussian integrated methods," *Eng. Anal. Bound. Elem.*, vol. 6, no. 2, pp. 66–71, 1989.
[17] A. H. Stroud, *Approximate Calculations of Multiple Integrals*. London: Princeton-Hall, 1971, p. 314.

A PC-Based Imaging System for Automated Platelet Identification

J.-S. Lin, C.-C. Tai, C.-W. Mao, C.-J. Jen, and K.-S. Cheng

***Abstract*—In this communication, a PC-based imaging system was developed for automatically identifying fluroscence-labeled individual platelets adherent to protein-coated surface under flow conditions. It is to eliminate the laborious and time-consuming task, and the subjective error of manual measurements. Based upon the features of adherent platelets, three passes of the image processing were developed for platelet identification. From the results, 90–95% accuracy could be routinely obtained. The platelet distribution and other related parameters could be easily extracted and investigated.**

Introduction

With the advance of the digital imaging microscopic technique, the studies of complex cellular functions and higher order structure analysis become easier, more objective, and more accurate [1]. A good survey of the objectives of microscopic image analysis appeared previously [2]. Most systems in the past were implemented with the minicomputers. Nowadays, with the rapid developments in VLSI and computer technologies, the PC-based imaging systems are available with low cost.

The microscopic visual inspection process using digital image processing plays an important role in hematological investigations, such as the tracking, counting, classification, and analysis of the white blood cells [3]–[5]. Other applications include the template matching for analyzing the intramembraneous particle distribution [6], and the interactive tracking of the platelets and polymorphonuclear leukocytes on biomaterial surfaces [5], [7]. Epifluorescence video microscopy, in particular, is a necessary tool for investigating the characteristics of adherent platelets in mural thrombogenesis [8]–[10]. In the study of the aggregation of platelets [9], the off-line digital image processing technique was developed for local measurements of the multiplatelet thrombi growth and distribution. However, due to the lack of the morphological information, there is only very limited success in automated identification of the fluorescence image of individual platelets. For all the analysis of platelet images, the identification is inevitably the first and most important step in digital image processing.

In this communication, a PC-based imaging system is employed for automated platelet identification using the image processing and pattern recognition techniques. The platelets adhered to the protein-coated surface under flow conditions could be identified and tracked dynamically. The interesting parameters, such as number of platelets per unit area, accumulation rate, adhesion status, and sustaining period, could also be extracted automatically.

System Description

An imaging system with a 80286-based personal computer (ARC Turbo-12) is used for automated platelet identification. The block-diagram of the whole experimental setup is shown in Fig. 1, which is similar to the one described by Hubble and McIntire [9]. A typical image grabbed from the tape of this imaging system is shown in Fig. 2. The flow direction is from right to left. The imaging card used for grabbing the image from either the video camera or video cassette recorder has the resolution of 512×512 with 256 gray levels (VFG-512, Visionetics, Taiwan, ROC). Other instruments included in the system are an epi-fluorescence microscope of Olympus (BH-2RFL), a video camera of Hamamatsu (C-2400-08), a flow chamber, a syringe pump, a dynamic image tracing system of Sony (BNU-820), and a time base corrector of Sony (BVT-800).

In this study, all the identification algorithms and subsequent analysis programs were implemented using the C language, and easily run on an IBM compatible microcomputer.

The whole blood drawn from a nonsmoking, nonmedicated healthy subject was used as the sample. In which, the fluorescent dye of acridine red (2 μM) and the anticoagulant of sodium cirate (0.32%) were added for specifically labeling the platelets and preventing it from clotting. The flow rate controlled by the syringe pump was set at 0.9 ML/min, with a corresponding surface shear rate of 445 s^{-1} to simulate arterial blood flow conditions.

Automated Platelet Identification

From the grabbed fluorescence image of platelets, most platelets identifiable by human eyes had their gray-level values higher than the neighborhood background by at least 20. As flow time increased, more and more platelets adhered to the protein-coated region but not to the uncoated portion of the glass. Therefore, the coating boundary became more and more distinguishable.

Manuscript received December 4, 1990; revised September 24, 1991. This work was supported in part by the National Science Council, R.O.C., under Grants of NSC76-0404-E006-14, NSC77-0404-E006-12, and NSC78-0412-B006-25.

J.-S. Lin, C.-C. Tai, and C.-W. Mao are with the Institute of Electrical Engineering, National Cheng Kung University, Tainan, Taiwan, R.O.C.
C.-J. Jen is with the Department of Physiology, National Cheng Kung University, Tainan, Taiwan, R.O.C.
K.-S. Cheng is with the Institute of Biomedical Engineering, National Cheng Kung University, Tainan, Taiwan, R.O.C.

IEEE Log Number 9201973.

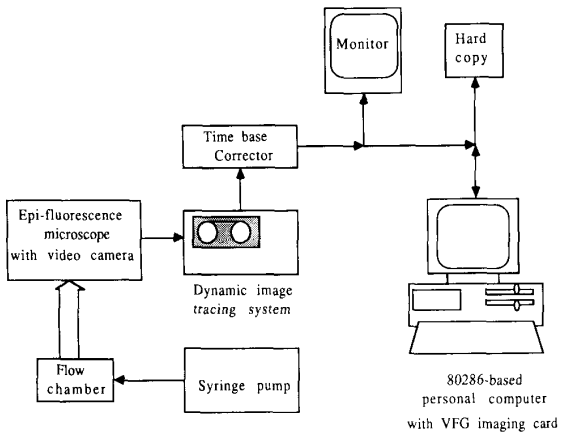

Fig. 1. Block diagram of system configuration.

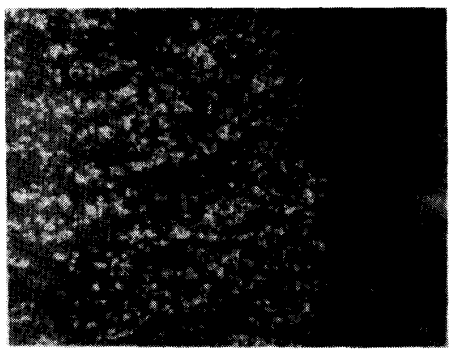

Fig. 2. Fluorescence micrograph of adherent platelets.

In practice, since the quality of the pictures, such as shown in Fig. 2, was good enough for the direct platelet identification without any preprocessing, both computation time and memory space for the PC-based imaging system were saved. To identify the locations of the center of adherent platelets, the algorithms of three passes were developed based upon the features of the fluorescent platelet image.

The histograms of the gray level in our pictures were nearly bimodal. Those pixels with high gray level values were mostly the platelets, and those with low values corresponding to the background. The method developed by Otsu [11] was adapted to perform automatic bilevel thresholding for later use. From this procedure, a background threshold was determined automatically. By carefully examining the gray level values of pixels for the individual platelets, the following information was obtained:

1) Most platelets had a diameter ranging from D_1 to D_2 pixels, which depending upon the amplification of the microscope.
2) Most platelets had a brighter central zone and a dimmer peripheral zone.
3) Most of the gray-level value differences between the central zone and the background threshold were larger than C_1.
4) Most of the gray-level value differences between the peripheral zone and the background threshold were larger than $C_2(C_2 < C_1)$.

Based upon the above information, "Pass 1" algorithm (Fig. 3) was developed for platelet identification. At least 80% of the adherent platelets could be detected using this algorithm. For the detection of smaller and dimmer platelets, a "Pass 2" algorithm was applied subsequently. "Pass 2" was similar to "Pass 1" except that it had a reduced diameter value and a reduced gray-level range of platelet. After being processed by the "Pass 1" and "Pass 2" algorithms, the leftover platelets could be identified by taking their radial properties into consideration—"Pass 3" algorithm (Fig. 4). Since these platelets were the dimmest among all, the "Pass 3" algorithm would search the pixels having the gray level greater than the background threshold by $C_3(C_3 < C_2)$. When necessary, based upon the histogram of platelets identified during the first round, the refined threshold could be obtained automatically and adapted for the second round identification process. The final result of the identified platelets were marked on the original picture for comparison in Fig. 5. The values of platelet diameter for $D1$ and $D2$, and the gray-level differences above the background threshold for C_1, C_2, and C_3, could be experimentally determined with iterative local histogram processing for each frame. However, in the same set of experiments, satisfactory results could be obtained using the same values for analyzing any frame.

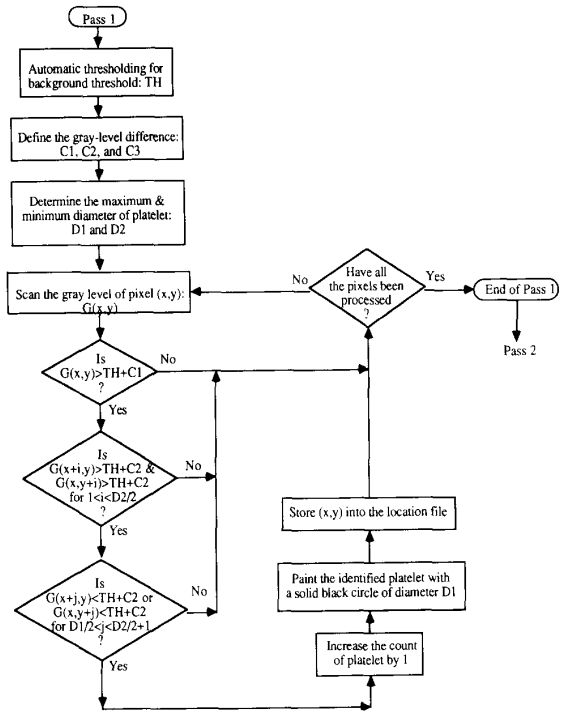

Fig. 3. Algorithm for platelet identification PASS 1.

Discussion and Application

Using the described procedures, 90–95% of identification accuracy could be routinely obtained. Moreover, excluding the preprocessing, as many as 1000 platelets could be easily identified within 1 min. In comparison, it usually took about 6 min for a person to count this many platelets, and the variation of results from person to person might be up to 20% (Table I). Although, the results from repeated counting by the same person was more reproducible, it is very tiresome for human to count more than five frames continuously without any break. Moreover, in our method not only the number of adherent platelets but also their respective locations

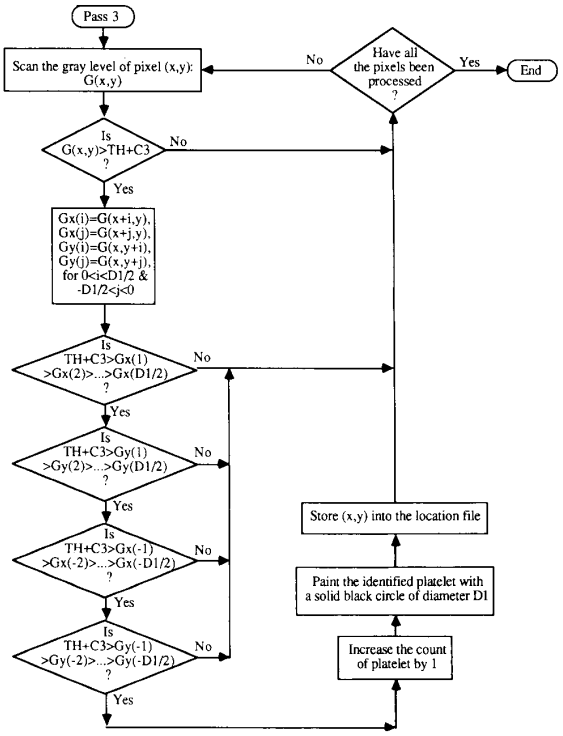

Fig. 4. Algorithm for platelet identification PASS 3.

Fig. 5. Platelets identified on the original picture.

could be obtained for analysis. A location file for each processed frame was saved for analyzing the adherent platelet distribution. Interesting parameters, such as number of adherent platelets per unit area, accumulation rate, adhesion status, sustaining period, could also be extracted automatically.

Table II represents the analysis of a typical set of results obtained from exposing the whole blood with fibrin coated surface. In this experiment, the D_1 and D_2 were set at 8 and 6 pixels, respectively. The parameters for C_1, C_2, and C_3 of three passes were 25, 20, and 15 in gray levels. The neighboring distance was defined as 8 pixels. The platelets identified by this automatic procedure was in good agreement with the manual measurements. Up to 3 min of blood exposure time, there were about 600 platelets adhered onto an area of 20 000 μm^2. Almost half of them had immediately adjacent neighbor(s). In addition, based upon the statistical analysis [12], it is also shown that the platelets initially adhered randomly but finally became uniformly distributed. This analysis indicates that the deposition of each platelet was an independent process, i.e., the adhered platelets did not influence the adhesion of incoming platelets. Therefore, we can provide this important information for blood physiologists regarding the dynamic behavior of platelet-fibrin interaction under flow.

Besides the single frame analysis, the frame-to-frame comparison could also be carried out in time sequence along the same experiment. Three types of adhesion status could be obtained: 1) newly attached platelets were the ones appearing on the location file $t2$ but not on the location file $t1$ ($t1$ and $t2$ were blood-surface contact times of the same experiment, and $t1 < t2$); 2) just de-

TABLE I
MANUAL MEASUREMENTS OF THE PLATELETS FOR THE FRAME SHOWN IN FIG. 2 BY SIX DIFFERENT PERSONS

Person	Meas. #1	Meas. #2	Meas. #3	Meas. #4	Meas. #5	Mean ± SD	Time
A	810	926	1130	1360	1196	1084 ± 218	5′28″
B	689	740	721	724	779	731 ± 33	5′08″
C	668	609	631	656	692	651 ± 32	3′25″
D	766	767	828	915	948	845 ± 84	3′34″
E	673	680	728	726	641	690 ± 37	3′02″
F	616	584	576	574	554	581 ± 23	4′06″

1) Count by the computer = 653 platelets/frame, time = 55 s.
2) The mean and standard deviation of all the measurements are 764 ± 190 platelets/frame.
3) The values shown in the last column "Time" are the mean time for five consecutive measurements.
Since practically each frame is counted only once by manual measurement, we take the average of the first count from each person as the "gold standard." The mean and the standard deviation for the first count of six persons are 704 ± 71 platelets/frame.

TABLE II
SINGLE FRAME ANALYSIS OF PLATELET ADHESION ONTO FIBRIN-COATED SURFACE AT 445 s^{-1} SURFACE SHEAR RATE

Time (sec)	Platelet per 20,000 μm^2*	Platelets with Neighbors**	Distribution
10	18	0	Random
20	44	6	Random
30	78	12	Random
40	119	24	Random
50	156	29	Random
60	209	44	Random
70	266	79	Random
80	308	85	Random
90	353	116	Random
100	377	135	Clustering
110	419	143	Random
120	474	214	Random
130	524	262	Random
140	554	253	Random
150	580	275	Random
160	605	287	Random
170	606	249	Uniform
180	650	286	Uniform

*The identification parameters were: $D_1 = 8$, $D_2 = 6$, $C_1 = 25$, $C_2 = 20$, and $C_3 = 15$.
**The neighboring distance was set at $D_1 = 8$.

tached platelets were the ones appearing on the location file $t1$ but not on the location file $t2$; and 3) staying platelets were the ones appearing on both location files. After comparing the location files in sequence, the curves for accumulative growth, staying, newly attached and detached cells could be obtained simultaneously.

ACKNOWLEDGMENT

The authors wish to thank Dr. C. F. Lam of Medical University of South Carolina, Charleston, for his kind suggestions and encouragement, and the authors are also grateful to J.-C. Sheu in preparation for this manuscript.

REFERENCES

[1] D. J. Arndt-Jovin, M. Robert-Nicoud, S. J. Kaufman, and T. M. Jovin, "Fluorescence digital imaging microscopy in cell biology," *Science*, vol. 230, no. 4723, pp. 247–256, Oct. 1985.
[2] P. H. Bartels and G. L. Wied, "Computer analysis and biomedical interpretation of microscopic images: current problems and future directions," *Proc. IEEE*, vol. 65, no. 2, pp. 252–261, Feb. 1977.
[3] M. D. Levine, Y. M. Youssef, P. B. Noble, and A. Boyarsky, "The quantification of blood cell motion by a method of automatic digital picture processing," *IEEE Trans. Patt. Anal. Mach. Intell.*, vol. PAMI-2, pp. 444–450, Sept. 1980.
[4] F. P. Ferrie, M. D. Levine, and S. W. Zucker, "Cell tracking: A modeling and minimization approach," *IEEE Trans. Patt. Anal. Mach. Intell.*, vol. PAMI-4, pp. 277–290, May 1982.
[5] R. A. Maludzinski, D. W. Capson, and I. A. Feuerstein, "Computer tracking of white blood cells on protein-coated surfaces," *IEEE Trans. Instrum. Meas.*, vol. IM-36, pp. 928–933, Dec. 1987.
[6] H. Frey, "Automatic measurement of intramembraneous particle distribution by digital image processing," *IEEE Trans. Biomed. Eng.*, vol. BME-34, pp. 553–555, July 1987.
[7] D. W. Capson, R. A. Maludzinski, and I. A. Feuerstein, "Microcomputer-based interactive tracking of blood cells at biomaterial surfaces," *IEEE Trans. Biomed. Eng.*, vol. BME-36, pp. 860–864, Aug. 1989.
[8] G. A. Adams and I. A. Feuerstein, "Visual fluorescent and radioisotopic evaluation of platelet accumulation and embolization," *Trans. Am. Soc. Artif. Intern. Organs*, vol. 26, pp. 17–23, 1980.
[9] J. A. Hubble and L. V. McIntire, "Technique for visualization and analysis of mural thrombogenesis," *Rev. Sci. Instrum.*, vol. 57, pp. 892–897, 1986.
[10] G. A. Adams, S. J. Brown, L. V. McIntire, S. G. Eskin, and R. R. Martin, "Kinetics of platelet adhesion and thrombus growth," *Blood*, vol. 62, pp. 69–74, 1983.
[11] N. Otsu, "A threshold selection method from gray-level histograms," *IEEE Trans. Syst., Man, Cybern.*, vol. SMC-9, pp. 62–68, Jan./Feb., 1979.
[12] J. H. Zar, "The Poisson distribution and randomness," in *Biostatistical Analysis*, Englewood Cliffs, NJ: Prentice-Hall, 1984, ch. 23, pp. 406–421.